Role of Mitophagy-based TLR9 Signal Pathway in Neonatal Ventilator-induced Lung Injury

Jinni Chen[1#], Dawei Li[2#*], Zhenzhen Huang[1], Caixia Zheng[1], Qiuyu Lin[1], Naichao Feng[1], Siqi Chen[1], Xiaolin Cao[2]

[1]*Department of Respiratory, Hainan Maternal and Children's Medical Center, Haikou, 570206, China*
[2]*Department of Endocrinology, The First Affiliated Hospital of Hainan Medical University, Haikou, 570102, China*
#These authors contributed equally to this work as co-first author

ARTICLE INFO

ABSTRACT

The study focused on the role of mitophagy in neonatal ventilator-induced lung injury (VILI). Immunoassays were used to study the TLR9 signaling pathway of neonatal VILI, expected to provide a feasible solution for neonatal VILI. The mice were randomly divided into four groups, group A: spontaneous breathing group; group B: normal tidal volume (VT) group (VT=9mL/kg); group C: high VT group (VT=39mL/kg); and group D: ODN2088 (400μg/ Only) intervention + high VT group. The four groups were compared for the expression of inflammatory factors. It was found that as the culture time increased, the expression of TLR9, MyD88, and NF-κBp65 in the lung tissue of the large VT group was significantly higher than those in the spontaneous breathing group and normal VT group, and the differences were statistically significant; and TLR9 inhibitors could activate the TLR9-MyD88 signaling pathway to up-regulate the expression of NF-κB, mediating the release of inflammatory factors to cause VILI.

Introduction

Mechanical ventilation can effectively reduce acute lung injury/acute respiratory dyspnea syndrome (ALI/ARDS). A respirator helps to maintain the patency of the respiratory tract and prevent harmful gases and carbon dioxide from accumulating in the lungs (1). However, despite the use of mechanical ventilation, the morbidity and mortality of severe patients are still high, and the use of mechanical ventilation can also cause lung injury or aggravate the condition (2). Ventilator-induced lung injury (VILI) is one of the most serious complications in the treatment of patients with mechanical ventilation. Therefore, the generation and progression mechanism of VILI is the focus of scholars (3).

Studies have found that the main causes of VILI include mechanical damage, biological damage, and their combined effects. Mechanical damage is mainly collision damage, air pressure damage, shear damage, etc. (4). Excessive breathing during mechanical ventilation will cause an excessive increase in lung volume and over-expansion of lung tissue, which is called severe osmotic pulmonary edema. Convolution is high airway pressure in artificial respiration arising from high cross-lung pressure (5). The main clinical symptoms include pneumothorax, mediastinal emphysema, and interstitial emphysema. During mechanical ventilation, the opening and closing of the small airways are repeated, increasing the damage to the alveolar epithelial cells. Even under proper conditions, mechanical damage will eventually lead to biological damage (6). Thanks to the abnormal mechanical pressure of lung tissue, intracellular signal transmission is activated, which causes systemic inflammation by promoting the inflammatory invasion of the lung, ultimately causing damage to multiple organs of the body (7).

The main cause of VILI is extensive destruction of the alveolar epithelium and vascular endothelium. As a result, transparency of alveolar capillary membranes increases, pulmonary edema and hemorrhage occur, glass membrane forms, and inflammatory cell infiltration increases. There are 13 Toll receptors (TLR) in mammals, and 1 to 10 TLRs appear in

---

humans. As an important pattern recognition receptor, TLR binds to various immune executive cells, such as epithelial cells, endothelial cells, and dendritic cells, and plays an important role in regulating innateness and acquiring immunity (8,9). There are 13 Toll receptors (TLR) in mammals and 1 ~ 10 TLRs in humans. As an important type of pattern recognition receptor, TLR is discovered by various immune executive cells such as epithelial cells, endothelial cells, and dendritic cells and plays an important role in regulating innateness and gaining immunity (8, 9). Studies have shown that in TLR families other than the TLR family, other TLRs induce myelodifferentiation factor 88 (MyD88)-dependent pathways. The activation of NF-κB induces the secretion of downstream inflammatory factors (10, 11).

Mitochondria are an important part of eukaryotes and provide the necessary main energy for cell life activities. Mitochondria have a specific phospholipid bimolecular membrane structure, and the deoxyribose ribose contained in the matrix wrapped by the inner membrane is the main genetic material of mitochondria, namely mitochondrial DNA (mtDNA) (12). Mitophagy is the selective autophagy degradation of mitochondria under damaged or stressed conditions by cells to maintain cell homeostasis and mitochondrial renewal and prevent damaged mitochondria from releasing a large amount of ROS and oxygen free radicals to damage cells. mtDNA has unmethylated citrulline (CpG) similar to bacterial DNA in structure. Scholars have found that mtDNA containing CpG is a risk-associated molecular model, and cellular tlr9 can specifically recognize it (13). The subsequent "cascade" inflammation leads to VILI (14). Nevertheless, the mechanism of activating VILI's inflammatory response is unknown. therefore, in this study, a mouse model of VILI was established, aiming to explore the mechanism of the tlr9-myd88 signal transmission path in the occurrence of VILI, and provide an evidence-based basis for clinical prevention and treatment of neonatal VILI.

Materials and methods
Research subjects

40 newborn mice were used. They weighed about 20 g. The average weight was 250 ± 20 g, and the animal certificate number was SCXK 2015-0002. All rats were domesticated in the laboratory for two weeks before the experiment, and the indoor temperature was 22°C ~ 24°C to ensure that the mice were free to eat and drink. Inclusion criteria: healthy and clean experimental mice purchased from Haikou Animal Experiment Center. The high-temperature and high-pressure sterilization method were used to sterilize and disinfect the utensils used. After the carotid catheter examination, 1 mL of blood was taken from each mouse to determine the plasma endotoxin content to rule out the influence of the infectious inflammations in the mice before the experiment.

VILI model

The mice were randomly divided into the following experimental groups (each group contained 10 mice). Group A: spontaneous breathing group; Group B: normal VT group (VT=9mL/kg); Group C: high VT group (VT=39mL/kg); group D: ODN2088 (400μg/head) intervention + high VT group (VT= 50mL/kg). Note: ODN2088 (500) μTLR9 inhibitor was administered for mice in group D. Two hours before endotracheal intubation, the mice were anesthetized. After anesthesia, the head and limbs were fixed. After a sterile cloth was applied in the surgical area, approximately 5mm of skin was cut on the skin sternum, and the subcutaneous tissue was peeled off to expose the trachea completely. After disinfection, a tracheotomy was performed, and the aseptic catheter (outer diameter 2.5mm) was fixed with a clean silk thread. Then, the femoral artery was separated, and the arterial pressure was measured by intubation. Next, the thigh vein of the mouse was isolated to establish venous access. During the experiment, the blood pressure and body temperature of the mice were maintained. This experiment was approved by the Society of Animal Ethics.

Collection and processing of serum

All mice were mechanically ventilated for 4 hours, and the chest and abdomen operation areas were disinfected with iodine 3 times. Then, the skin of the mice was cut until the heart was exposed. The experiment was under negative pressure. The needle tip and puncture depth were fixed after blood circulation was established. Then, the injection volume was gradually reduced, but the blood volume of the syringe should not change until the pressure

disappeared. 5-6mL of the liquid sample was transferred into a 10mL clean centrifuge tube, and the centrifugation parameters were: 4°C, 3000 plastic wraps, 10 minutes. After centrifugation, the hose was removed, and the upper layer was discarded with a pipette. Then, the serum was separated into 4 parts, which were labeled and stored at -80°C.

Detection of IL-6, IL-1β, and TNF-α in serum

ELISA was used to determine the inflammatory factors in the serum of mice. The relevant principles of the experiment were as follows. 1. Coating: on the cellulose acetate film, two substances that produce an immune response can be adsorbed. The solid carrier contains many large cavities, which can effectively adsorb antigens and antibodies (such as protein) and retain the stability, activity, hydrophobicity, and antigen-antibody property of biological macromolecules. 2. Labeling: the antigen or antibody can be conjugated with the catalytic substance to form a catalytic conjugate, and the enzyme complex can maintain immune activity and catalytic properties. 3 Color development: the enzyme conjugate is combined with the corresponding antigen or antibody covered in the solid phase carrier and fixed on the solid phase carrier. A color develops after the enzyme substrate is added. The relative content of the antigen or antibody can be calculated based on the color depth. The residual free reactants are then removed, and the substrate TMB is used for color rendering. Ethyl enzyme catalyzes the discoloration of TMB to blue, which finally turns blue to yellow in the presence of acid. Therefore, the concentration of the detected sample has a positive correlation with the depth of the color. After the reaction is over, the absorbance of the 450nm complex is measured with a microplate analyzer, the sample concentration is calculated, the OD value of each well is recorded, and the OD value of well S0 is subtracted from the OD value of each well to obtain the final result of the average value of the well. The curve is drawn using Origin, the horizontal axis is the standard product, and the vertical axis is the concentration of the standard substance. The regression formula of the standard curve is obtained as per the prompts of the software. In addition, the curve correlation coefficient R is greater than 0.95, and a result close to 1 as much as possible is considered to be excellent. The OD value

of each item will be substituted into the equation to calculate its concentration. If the liquid needs to be diluted, the concentration is multiplied by the corresponding dilution factor, and finally, the concentration of the sample is tested.

Detection of total protein content in BALF

Quantitative bronchoalveolar lavage fluid (BALF) is used to detect the total protein content of BALF. The copper ion divalent ion protein is reduced to the copper ion monovalent ion in an alkaline environment. The protein concentration is proportional to the degree of consistency of the light absorption intensity of the purple complex. After the reaction, the absorbance value or OD value of the complex at 562nm is determined by the microplate analyzer. The OD value of each well is recorded and the average of two wells is taken. The curve is drawn using Origin. The horizontal axis takes OD as the reference value, and the corresponding vertical axis is the standard concentration. A regression formula for calculating the standard curve has been proposed. The curve correlation coefficient R must be greater than 0.95. Then, the sample OD value is substituted into the formula to calculate the concentration of the test serum. If the liquid needs to be diluted, the concentration is multiplied by the corresponding dilution factor, and finally, the concentration of the sample is tested.

Determination of pulmonary edema

The upper lobe tissue of the right lung was separated, and the surface moisture was quickly dried with clean filter paper. Then, it was placed on a precision electronic balance to measure the wet weight (W). Next, it was transferred to a drying oven at 60 °C for two days to reach the required dry weight. The mass is set as dry mass (d), and the specific gravity of the lung moist/dry (w/d) is calculated. The pathology of the lungs was observed using the hematoxylin-eosin (HE) staining method. The cytoplasm contains a lot of basic proteins which combine with acid pigments to produce chromic acid deoxyribonucleic acid. This is the main transport material and can be combined with alkaline epoxy resin to become blue-violet. The color contrast can be observed through the optical microscope.

Immunohistochemical detection of TLR9, MyD88, and NF-kB

Immunohistochemistry is an experimental operation based on immunological antigen and antibody reactions. The resistance uses a specific combination of antigens and antibodies, and a certain chemical is used as a coloring agent. This reaction turns the color body into an antibody color body. The lung tissue can be checked by an optical microscope and the antigen binding to the colored antibody is sensitive and specific, which can be used in qualitative and quantitative chemical research.

Quantitative analysis of TLR9, MyD88, and NF-kB

The Western Blot method is used for immunohistochemical detection. Anti-LC3B Rabbit antibody (Cell Signaling Technology) protein molecular weight was 80 - 140 kDa: 8%; 25 - 80 kDa: 10%; 15 - 40 kDa: 12%; < 20 k Da: 15%, leak test before filling. Polyacrylamide gel electrophoresis is a frequently used electrophoresis medium that contains polyacrylamide gel and detergent. Detergent (SDS) can remove the charge of biological macromolecules. The protein is detected by the primary antibody and the colored secondary antibody in separate steps. The electrophoresed molecules are placed on the solid-phase carrier according to the molecular weight, excluding short non-protein peptides and only adsorbing protein substances. The protein or polypeptide on the cellulose acetate film is used as an antigen and the corresponding antibody binds to the color-developing substance. The secondary antibody is labeled with an enzyme or isotope, and the matrix chromosome or optical imaging is used to detect the protein composition expressed by the specific target gene. The basic idea is to use a secondary antibody labeled with an antibody, a "probe" to develop color. SDS polyacrylamide gel electrophoresis uses the molecular weight protein as an antigen and transfers it to the PVDF membrane solid-phase carrier. After the corresponding resistor reaction, it reacts with the enzyme or isotope-labeled secondary antibody. Finally, the ECL monitor obtains the target protein in the detected tissue through the developing device.

Measurement of the level of mitochondrial phagocytosis

Mitochondrial autophagy was undertaken as the gold standard for observing mitochondrial autophagy. Through transmission electron microscopy, it can be observed that the mitochondria gathered around the cell nucleus; mitochondria appeared to be swelling and degenerating, and there was a bubble-like double membrane structure around it; the double membrane structure wrapped the swollen and denatured mitochondria to form autophagosomes; the fusion of mitochondrial autophagosomes and lysosomes formed autophagolysosomes, and non-degradable mitochondrial remains were occasionally seen in autophagolysosomes.

Statistics

The data was processed by SPSS20.00 software. First, the Kolmogorov-Smirnov method was used to test the normality of the data. Each experiment was independently repeated more than three times. The Graphpad Prism 5.0 statistical software was used for statistical analysis. All data were expressed as mean±SEM. One-way analysis of variance analysis and Tukey's multiple comparison test were used, and $P<0.05$ was the threshold for significance.

Results and discussion
Comparison of inflammatory factors in mouse serum

The results showed that compared with groups A and B, the levels of IL-1β, IL-6 and TNF-α in the serum of the large VT group were significantly increased (all $P<0.05$); the expression of inflammatory factors in the serum of the mtDNA inhibitor group was significantly lower than that of the large VT group ($P<0.05$); there was no significant difference between groups A and B (all $P>0.05$), as shown in Figure 1.

Comparison of edema degree of lung tissue and total protein content in BALF

Compared with groups A and B, the large VT group had higher total protein content and W/D ratio, and the difference was statistically significant (all values $P<0.05$). The W/ D ratio and the total protein content in the TLR9 inhibitor group were significantly lower than those in the large VT group ($P<0.05$);

there was no significant difference between groups A and B (all $P>0.05$), as shown in Figure 2.
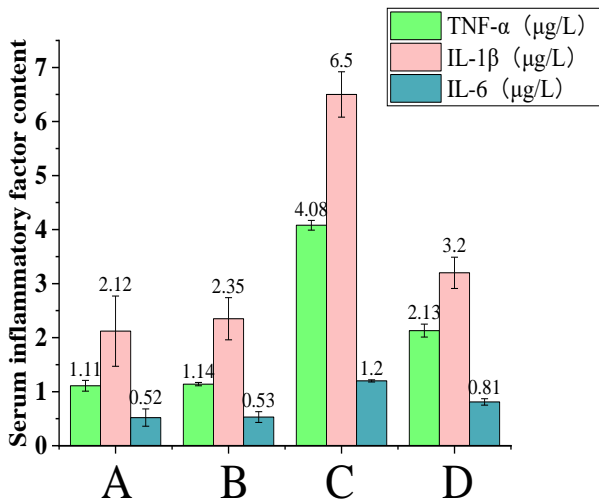
Figure 1. The effect of different tidal volumes (VT) on the content of serum inflammatory factors in mice. Note: the VT of the normal VT group was 8mL/kg, and the VT of the large VT group was 40mL/kg; IL-6 and IL-1β were referred to as interleukin-6 and interleukin-1β, and TNF-α was tumor necrosis factor-α. Compared with group A, $P<0.05$; compared with normal VT group, ($P<0.05$), compared with large VT group, it was not statistically significant ($P<0.05$).
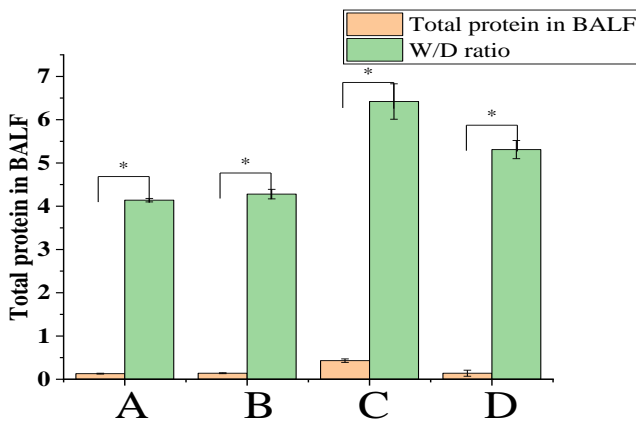

Figure 2. The effect of VT on the W/D ratio and the total protein content of BALF. (Note: W/D ratio was the wet/dry weight ratio, BLAF referred to bronchoalveolar lavage fluid; VT of group B was 8mL/kg, VT of large VT group was 40mL/kg; compared with group A ($P<0.05$); compared with group B, ($P<0.05$), compared with large VT group ($P<0.05$)

Mechanical ventilation-induced autophagy and autophagosome formation

VT=30 and 40mL/kg mechanical ventilation for more than 2.0h can significantly induce the increased expression of autophagy-related proteins. That is, autophagy is activated to a certain extent, but the formation of autophagosomes requires further TEM examination. TEM examination showed that typical autophagosomes were found in rat alveolar type II epithelial cells (at-iis) after VT=30mL/kg ventilation for 2.0h. Autophagosomes were further developed by VT=30mL/kg or ventilation for 3.0h to 4.0h. Autophagosomes form autophagolysosomes and degrade their contents. Different numbers of autophagosomes or autophagolysosomes were found in alveolar type I epithelial cells (Figure 3AB). The use of Tlr9 inhibitors significantly improved the pathological changes in lung tissue. The histological scores in the large VT group were significantly higher than those of group A, group B, and the Tlr9 obstruction group, but there was no significant difference between group A and group B ($P>0.05$) as shown in Figure 4.
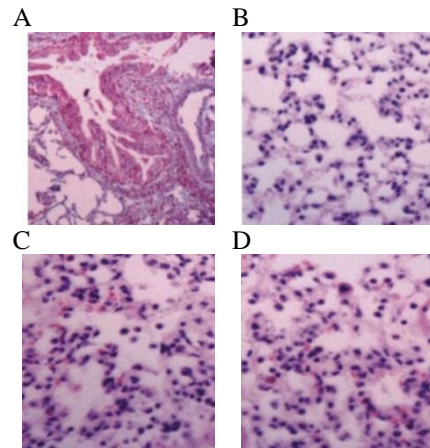

**Figure 3.** The HE staining of the pathological structure of lung tissue of mice in each group.
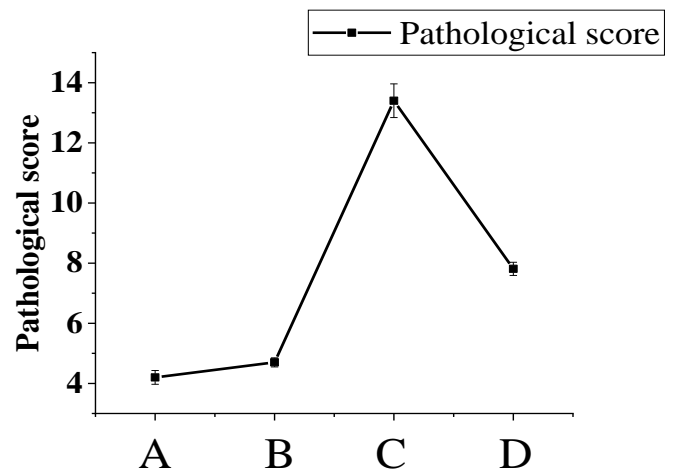
Figure 4. The effect of different VT on the pathological score of lung tissue in mice.

Comparison of immunohistochemical results of TLR9, MyD88, and NF-κB protein in lung tissue

The optical microscope showed that in the large VT group, the expression level of MyD88 and TLR9NF-κB65 in the lung tissue was higher than other factors. In addition, TLR9 inhibitors could reduce the levels of TLR9, MyD88, and NF-κB65 protein in groups A and B. Quantitative analysis showed that in the Tlr9 inhibitor group, the IVR score and the expression of the three factors were significantly higher versus the groups A and B ($P<0.05$). There was no statistically significant difference between groups A and B (all $P>0.05$), as shown in Figure 5 and Figure 6.
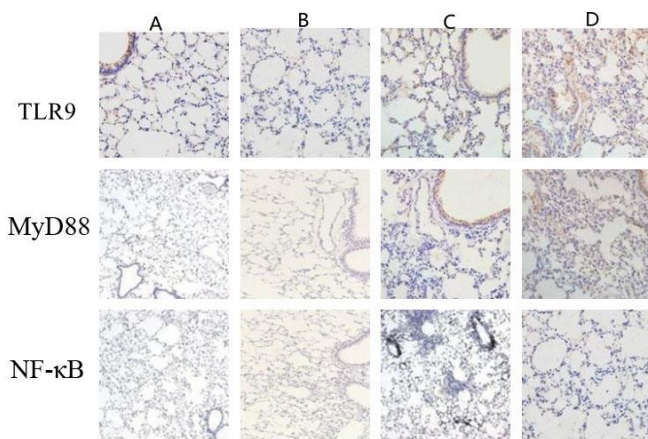

Figure 5. TLR9, MyD88, and NF-κB staining results.
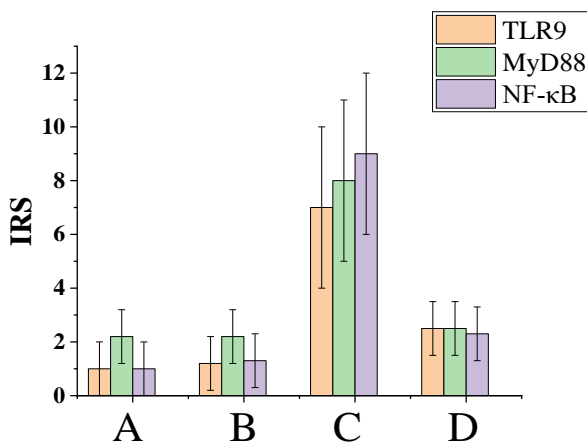
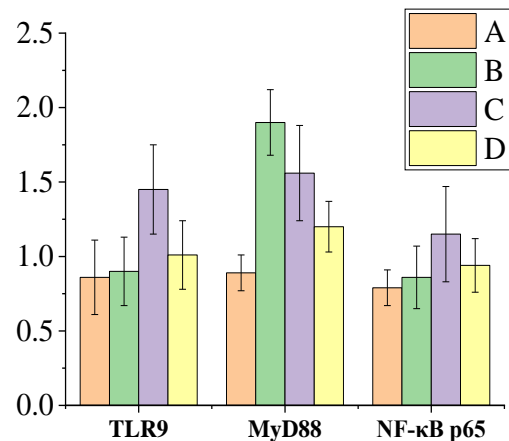**Figure 6.** IVR score of TLR9, MyD88, and NF-κB protein.

Comparison of Western Blot results of TLR9, MyD88, and NF-κB protein in lung tissue

The expression of TLR9, MyD88, and NF-κBp65 in the lung tissue of the large VT group was significantly higher than that in groups A and B , and the differences were statistically significant; and TLR9 inhibitor could reduce the expression of TLR9,

MyD88, and NF-κBp65 protein; and the difference between group A and group B was not statistically significant, as shown in Figure 7 and Figure 8.
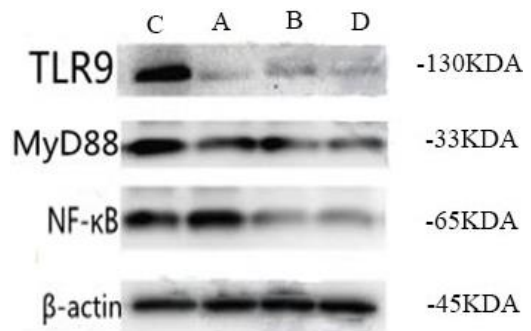
Figure 7. Western Blot results of TLR9, MyD88, and NF-κB protein.

Figure 8. Expression of TLR9, MyD88 and NF-κB protein.

With the development of science and technology, the birth rate and survival rate of premature infants have also been significantly improved (15). Due to the immature development of tissue and organs and the low adaptability to the extrauterine environment, various complications will occur. Most importantly, the lack of pulmonary surfactants leads to dyspnea syndrome after birth, which easily leads to insufficiency of breathing, and ultimately leads to multiple organ damage and death (16). Those with lower gestational age and weight have lower survival rates. Mechanical ventilation can maintain oxygen levels in the blood of premature infants. However, long-term mechanical ventilation causes severe lung injury, such as bronchial asthma (17). In order to reduce or avoid the serious injury caused by invasive ventilation, scholars began to study the related pathogenesis. Mitophagy selectively phagocytos and degrades damaged mitochondria, which may destroy

the integrity of the mitochondrial membrane and the escape of mtDNA into the cytoplasm and blood. The latest research proposes that mtDNA released by escape can be used as a risk-related molecular model (DAMP) in the cell to activate and regulate the innate immune response and inflammatory response to deal with various adverse factors inside and outside the cell. TLR9 recognizes its agonists and produces immune responses mainly through MyD88-dependent signal channels. MyD88 recruits IL-1R receptor-associated kinase-1 (IRAK-1) and IRAK-4 containing DD through its death domain (DD). IRAK-1 is the substrate of IRAK-4. It activates NF-κB by activating NF-κB. Transcription of downstream inflammatory cytokines such as IL-6, IL-12, TNF-α, and IFN-α. The activation of the TLR9-MyD88-NF-κB signal channel can initiate the transcription and synthesis of downstream inflammatory factors. A large number of studies have found that infections including bacteria, viruses and other pathogens are most closely related to the onset of HSP. After lung injury, the upstream TLR9-MyD88-NF-κB signal channel is activated, and the activated NF-κB induces the expression of a variety of downstream inflammatory factors, enzymes and other genes. Therefore, the pathogenesis of lung injury is closely related to the TLR9-My D88-NF-κB signal channel.

In the study, it was found that in the Tlr9 inhibitor group, the expression levels of MyD88 and NF-κB were significantly higher than the spontaneous breathing group and the normal VT group. At the same time, the levels of serum inflammatory factors (IL-6, IL-1β, and TNF-α) also increased. However, there was no significant difference between the spontaneous breathing group and the normal VT group. The TLR9 inhibitor ODN2088 significantly reduced the expression of TLR9, MyD88, and NF-κB and improved the inflammatory response in lung tissue. It suggested that mechanical ventilation mediated the production of VILI by activating THE tlr9-myd88 signaling pathway. The Toll receptor, known as the VIIL pattern recognition receptor, plays an important role in inducing innate immunity and inflammation (18,19). Previous studies have shown that the TLR9 receptor has a great correlation with innate immunity or acquired response. Activated TLR9 couples to downstream MyD88 molecules through the TIR, induces MyD88-dependent pathways

and activates NF-κB. As a result, the secretion of inflammatory factors IL-6, IL-1, and TNF-α is hindered (20). In this study, mitophagy was found to effectively reduce neonatal lung injury caused by mechanical ventilation, thereby reducing the production of MyD88 and NF-κB protein.

Conclusions

In the study, it was found that mechanical ventilation for 4 hours can cause mechanical damage to the lungs. Mitophagy can activate the TLR9-MyD88 signaling pathway. NF-κB is located downstream of the signaling pathway and is activated to produce an immune response, mediating the release of inflammatory factors and causing acute inflammation in lung tissue. Eventually, VILI occurs. However, some limitations should be noted in the study. This study only verifies the mechanism of mitophagy in affecting neonatal VILI. In the follow-up, an in-depth research is necessary to strengthen the findings of the study.

Interest conflict

The authors declare that they have no conflict of interest.

References

1. Tilstra JS, John S, Gordon RA, Leibler C, Kashgarian M, Bastacky S, Nickerson KM, Shlomchik MJ. B cell-intrinsic TLR9 expression is protective in murine lupus. J Clin Invest. 2020 Jun 1;130(6):3172-3187.
2. Zhou B, Yan J, Guo L, Zhang B, Liu S, Yu M, Chen Z, Zhang K, Zhang W, Li X,Xu Y, Xiao Y, Zhou J, Fan J, Hung MC, Li H, Ye Q. Hepatoma cell-intrinsic TLR9activation induces immune escape through PD-L1 upregulation in hepatocellularcarcinoma. Theranostics. 2020 May 17;10(14):6530-6543.
3. Liu Y, Nguyen PT, Wang X, Zhao Y, Meacham CE, Zou Z, Bordieanu B, Johanns M,Vertommen D, Wijshake T, May H, Xiao G, Shoji-Kawata S,

Rider MH, Morrison SJ,Mishra P, Levine B. TLR9 and beclin 1 crosstalk regulates muscle AMPK activationin exercise. Nature. 2020 Feb;578(7796):605-609.

4. Khan NS, Lukason DP, Feliu M, Ward RA, Lord AK, Reedy JL, Ramirez-Ortiz ZG,Tam JM, Kasperkovitz PV, Negoro PE, Vyas TD, Xu S, Brinkmann MM, Acharaya M,Artavanis-Tsakonas K, Frickel EM, Becker CE, Dagher Z, Kim YM, Latz E, PloeghHL, Mansour MK, Miranti CK, Levitz SM, Vyas JM. CD82 controls CpG-dependent TLR9signaling. FASEB J. 2019 Nov;33(11):12500-12514. Marongiu L, Gornati L, Artuso I, Zanoni I, Granucci F. Below the surface: Theinner lives of TLR4 and TLR9. J Leukoc Biol. 2019 Jul;106(1):147-160.

5. Reilley MJ, Morrow B, Ager CR, Liu A, Hong DS, Curran MA. TLR9 activationcooperates with T cell checkpoint blockade to regress poorly immunogenicmelanoma. J Immunother Cancer. 2019 Nov 26;7(1):323.

6. Ashley SN, Somanathan S, Giles AR, Wilson JM. TLR9 signaling mediatesadaptive immunity following systemic AAV gene therapy. Cell Immunol. 2019Dec;346:103997.

7. Makita Y, Suzuki H, Kano T, Takahata A, Julian BA, Novak J, Suzuki Y. TLR9activation induces aberrant IgA glycosylation via APRIL- and IL-6-mediatedpathways in IgA nephropathy. Kidney Int. 2020 Feb;97(2):340-349.

8. Liu FY, Fan D, Yang Z, Tang N, Guo Z, Ma SQ, Ma ZG, Wu HM, Deng W, Tang QZ.TLR9 is essential for HMGB1-mediated post-myocardial infarction tissue repairthrough affecting apoptosis, cardiac healing, and angiogenesis. Cell Death Dis.2019 Jun 17;10(7):480.

9. Wei W, Ren J, Yin W, Ding H, Lu Q, Tan L, Deng S, Liu J, Yang Q, Wang J,Wang M, Yue Y, Hao L. Inhibition of Ctsk modulates periodontitis with arthritisvia downregulation of TLR9 and autophagy. Cell Prolif. 2020 Jan;53(1):e12722.

10. Sharma S, Aldred MA. DNA Damage and Repair in Pulmonary ArterialHypertension. Genes (Basel). 2020 Oct 19;11(10):1224.

11. Zhao D, Li Y, Peng C, Lin J, Yu F, Zhao Y, Zhang X, Zhao D. Outer membraneprotein a in Acinetobacter baumannii induces autophagy through mTOR signallingpathways in the lung of

SD rats. Biomed Pharmacother. 2021 Mar;135:111034.

12. Druck T, Cheung DG, Park D, Trapasso F, Pichiorri F, Gaspari M, Palumbo T,Aqeilan RI, Gaudio E, Okumura H, Iuliano R, Raso C, Green K, Huebner K, CroceCM. Fhit-Fdxr interaction in the mitochondria: modulation of reactive oxygenspecies generation and apoptosis in cancer cells. Cell Death Dis. 2019 Feb15;10(3):147.

13. Gattinoni L, Tonetti T, Cressoni M, Cadringher P, Herrmann P, Moerer O, Protti A, Gotti M, Chiurazzi C, Carlesso E, Chiumello D, Quintel M. Ventilator-related causes of lung injury: the mechanical power. Intensive Care Med. 2016;42(10):1567-1575.

14. Jobe AH. Mechanisms of Lung Injury and Bronchopulmonary Dysplasia. Am JPerinatol. 2016 Sep;33(11):1076-8.

15. Kalikkot Thekkeveedu R, Guaman MC, Shivanna B. Bronchopulmonary dysplasia: Areview of pathogenesis and pathophysiology. Respir Med. 2017 Nov;132:170-177.

16. Sexauer W, Woodford M, Pack K, Allen A, Crawford A, Rakocevic G. Dyspnea in Patients with Stiff-Person Syndrome. Am J Med Sci. 2019 Oct;358(4):268-272.

17. Syed MA, Shah D, Das P, Andersson S, Pryhuber G, Bhandari V. TREM-1Attenuates RIPK3-mediated Necroptosis in Hyperoxia-induced Lung Injury inNeonatal Mice. Am J Respir Cell Mol Biol. 2019 Mar;60(3):308-322.

18. Tracy MK, Berkelhamer SK. Bronchopulmonary Dysplasia and Pulmonary Outcomes of Prematurity. Pediatr Ann. 2019 Apr 1;48(4):e148-e153.

19. Lal CV, Ambalavanan N. Maternal antibiotics augment hyperoxia-induced lunginjury in neonatal mice. Am J Physiol Lung Cell Mol Physiol. 2020 Feb1;318(2):L405-L406.

20. Hwang JS, Rehan VK. Recent Advances in Bronchopulmonary Dysplasia:Pathophysiology, 1Prevention, and Treatment. Lung. 2018 Apr;196(2):129-138.

21. Dennery PA. Heme oxygenase in neonatal lung injury and repair. Antioxid RedoxSignal. 2014 Nov 1;21(13):1881-92.